LASER INTERFEROMETER GRAVITATIONAL WAVE OBSERVATORY
-LIGO-
CALIFORNIA INSTITUTE OF TECHNOLOGY
MASSACHUSETTS INSTITUTE OF TECHNOLOGY

Technical Note	**LIGO-T040010- 00- R**	2/5/04

Signal Extraction Matrix of the 40m Detuned RSE Prototype

S. Kawamura

This is an internal working note
of the LIGO Project.

California Institute of Technology
LIGO Project – MS 51-33
Pasadena CA 91125
Phone (626) 395-2129
Fax (626) 304-9834
E-mail: info@ligo.caltech.edu

Massachusetts Institute of Technology
LIGO Project – MS 20B-145
Cambridge, MA 01239
Phone (617) 253-4824
Fax (617) 253-7014
E-mail: info@ligo.mit.edu

WWW: http://www.ligo.caltech.edu

ABSTRACT

Some results on the simulated signal extraction matrix of the 40m detuned RSE in the stationary case obtained using FINESSE are presented. The analyses include the following: comparison between the differential demodulation and double demodulation, dependence of the interferometer length signals and dc offset on the demodulation phases of the double demodulation, the port allocation for obtaining optimum length signals, comparison of the three pick-off ports, and effect of the macroscopic cavity length offset on the signal matrix.

1. Introduction

The signal extraction method for the 40m detuned Resonant Sideband Extraction (RSE) prototype is described in the "Conceptual Design of the 40meter Laboratory Upgrade for prototyping a Advanced LIGO Interferometer" (LIGO-T010115-00-R). The default design is to extract the interferometer length signals using two phase modulations. The method and the signal matrix obtained using TWIDDLE are shown in Table 1 and Fig.1.

Table 1. Signal extraction matrix of the 40m detuned RSE prototype.
(Upper: Raw value; Lower: Normalized)

Port	**Dem. Freq.**	L_+	L_-	l_+	l_-	l_s
SP	f_1	**1.5E+1**	**0**	**-6.2E-2**	**6.4E-2**	**-1E-3**
AP	f_2	**0**	**1.69**	**0**	**2E-3**	**0**
SP	$f_2 - f_1$	**-3E-4**	**1E-4**	**2.1E-1**	**2.9E-2**	**3.9E-2**
AP	$f_1 \times f_2$	**0**	**0**	**2.5E-3**	**-3.4E-3**	**-4E-4**
PO	$f_2 - f_1$	**5E-3**	**-4E-3**	**1**	**-2.8E-1**	**-3.0**

Port	**Dem. Freq.**	L_+	L_-	l_+	l_-	l_s
SP	f_1	**1**	**0**	**-4.1E-3**	**4.2E-3**	**-7E-5**
AP	f_2	**0**	**1**	**0**	**1E-3**	**0**
SP	$f_2 - f_1$	**-1E-3**	**5E-4**	**1**	**1.4E-1**	**1.8E-1**
AP	$f_1 \times f_2$	**0**	**0**	**-7.3E-1**	**1**	**-1E-1**
PO	$f_2 - f_1$	**-2E-3**	**1E-3**	**-3E-1**	**9.3E-2**	**1**

Here SP, AP, and PO stand for symmetric port, asymmetric port, and pick-off port, respectively. L_+, L_-, l_+, l_-, and l_s are length signals defined in Fig. 1. f_1 and f_2 are frequencies of the two phase modulations. Demodulation of $f_2 - f_1$ indicates differential demodulation and that of $f_1 \times f_2$ is double demodulation.

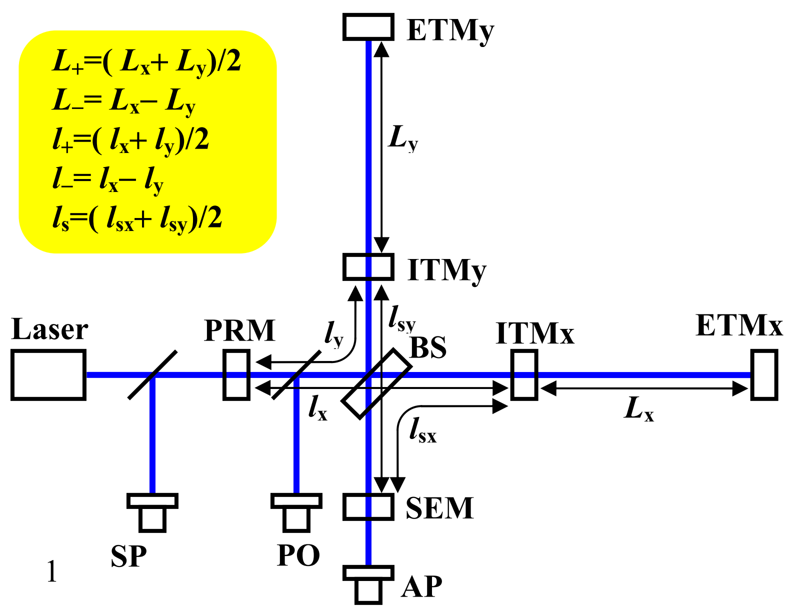

Fig. 1. Optical configuration of the 40m prototype.

In this new document the signal extraction method and matrix established in the previous document will be further refined using FINESSE.

2. Comparison between differential demodulation and double demodulation

Since double demodulation has two adjustable parameters (demodulation phases) while differential demodulation has only one, it could be possible to produce a better signal matrix with the double demodulation. Table 2 compares the signal matrix obtained by double demodulation with that by differential demodulation.

Here the demodulation phase for the differential demodulation is optimized to remove dc offset. The demodulation phases for double demodulation are optimized to remove dc offset and to maximize the desired length signal. This kind of optimization for demodulation phases of the double demodulation is used throughout this document. PO is the port for the light coming from BS to one of the ITMs.

Table 2. Comparison between double demodulation and differential demodulation.
(Upper: Raw value; Lower: Normalized; Yellow zone indicates double demodulation.)

Port	Dem. Freq.	Dem. Phase	L_+	L_-	l_+	l_-	l_s
SP	$f_2 - f_1$	22	6.2E-6	1.7E-6	-3.6E-3	5.2E-4	4.1E-4
SP	$f_1 \times f_2$	189,32	-1.3E-5	-2.3E-6	7.8E-3	-2.5E-4	-8.2E-4
AP	$f_2 - f_1$	111	-1.1E-6	-9.4E-7	-2.0E-4	-5.3E-5	-3.1E-4
AP	$f_1 \times f_2$	4,81	8.9E-8	-2.1E-7	-1.1E-4	-1.4E-4	-1.0E-5
PO	$f_2 - f_1$	208	6.0E-5	5.2E-5	1.0E-2	3.5E-3	1.8E-2
PO	$f_1 \times f_2$	164,12	1.3E-4	9.7E-5	1.7E-2	-8.2E-4	3.6E-2

Port	Dem. Freq.	Dem. Phase	L_+	L_-	l_+	l_-	l_s
SP	$f_2 - f_1$	22	-1.7E-3	-4.6E-4	1	-1.4E-1	-1.1E-1
SP	$f_1 \times f_2$	189,32	-1.7E-3	-3.0E-4	1	-3.2E-2	-1.0E-1
AP	$f_2 - f_1$	111	2.0E-2	1.8E-2	3.7	1	5.8
AP	$f_1 \times f_2$	4,81	-6.2E-4	1.5E-3	7.5E-1	1	7.1E-2
PO	$f_2 - f_1$	208	3.4E-3	3.0E-3	5.9E-1	2.0E-1	1
PO	$f_1 \times f_2$	164,12	3.6E-3	2.7E-3	4.6E-1	-2.3E-2	1

It can be seen from Table 2 that the cross-coupling of the l_- signal obtained at AP is significantly improved by employing the double demodulation (See the blue numbers). And for the l_+ signal obtained at SP and the l_s signal obtained at PO, some improvements are obtained by the double demodulation (See the green numbers).

Since our circuit design for the photodetector and demodulation system allows both double demodulation and differential demodulation (we can switch from one to the other just by changing a relevant parameter in a computer), it would not be a bad idea to use double demodulation for all the three length signals, l_+, l_-, and l_s. We use this convention for the rest of the document.

2. Dependence of each DOF on demodulation phases

The demodulation phases for the double demodulation are optimized to remove the dc offset and maximize the desired length signal. Here the contour plots for the l_+, l_-, and l_s signals and dc offset at the three ports, SP, AP, and PO are shown in Fig. 2 to Fig. 4.

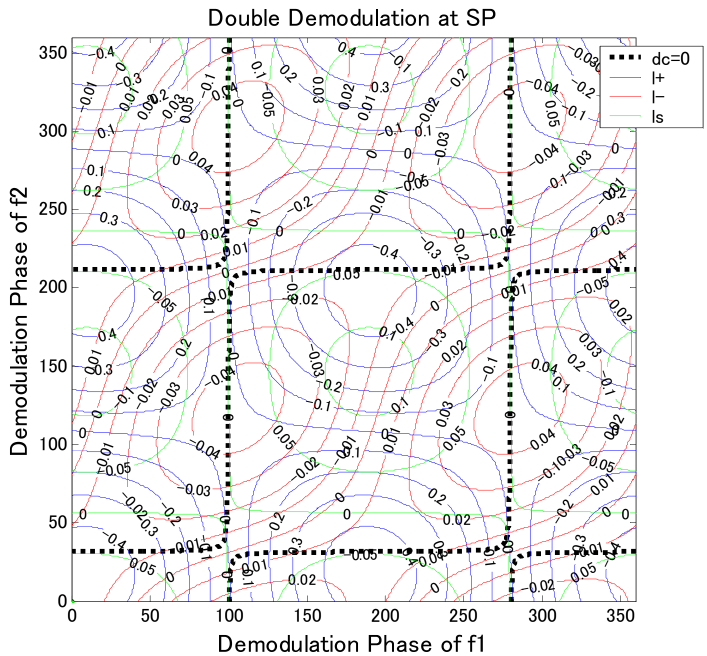

Fig. 2. Dependence of the signals and dc offset at SP on the demodulation phases.

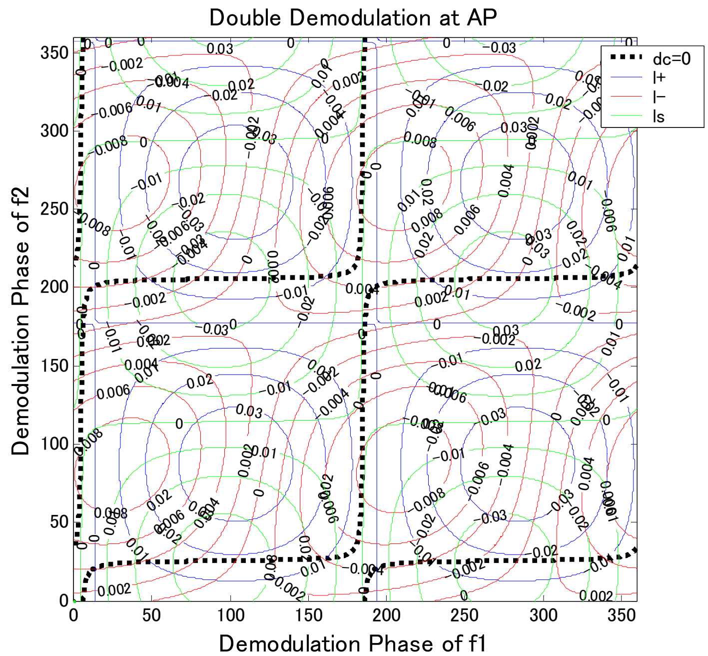

Fig. 3. Dependence of the signals and dc offset at AP on the demodulation phases.

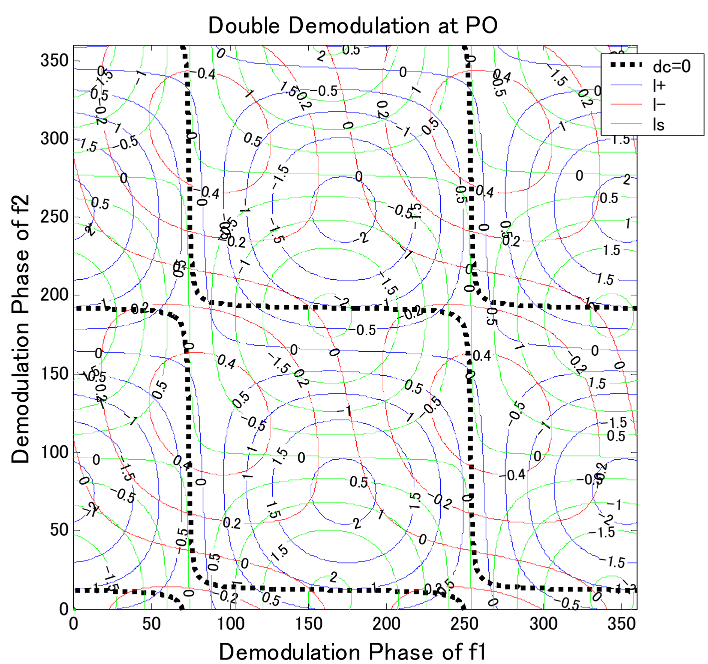

Fig. 4. Dependence of the signals and dc offset at PO on the demodulation phases.

To optimize the demodulation phases, one has to find a pair of demodulation phases that is on the dotted black line (dc=0) and is also close to the top (or bottom) of the desired signal contour. The question is whether that point is close to zero for the other DOFs. From the figures, it can be seen that there are such points for l_+ and l_- at SP, l_- and l_s at AP, and l_- and l_s at PO.

3. Allocation of ports for optimal signals

The signal matrix obtained with this kind of optimization for the double demodulation phases for all the possible port-signal allocations is shown in Table 3.

It can be seen from Table 3 that the l_+ signal can be obtained at SP, l_- at SP, AP, and PO, and l_s at AP and PO with relatively good cross-coupling. (There are only three poor ports a given signal, which are highlighted in red.) Here the criteria for a good cross-coupling is defined that any cross-coupling is less than unity for the normalized matrix. Although the port allocation of l_+ at SP, l_- at PO, and l_s at AP is satisfactory, comparable with the default design (l_+ at SP, l_- at AP, and l_s at PO), we would stick to the default design without any particularly strong reason.

Table 3. Comparison of the three ports for obtaining the l_+, l_-, and l_s signals
(Upper: Raw value; Lower: Normalized; Yellow zone indicates default design.)

Desired DOF	Port	Demod. Phase	L_+	L_-	l_+	l_-	l_s
l+	SP	189,32	-1.3E-5	-2.3E-6	7.8E-3	-2.5E-4	-8.2E-4
	AP	104,26	2.2E-6	1.7E-6	3.1E-4	5.5E-7	6.0E-4
	PO	177,12	1.2E-4	9.3E-5	1.7E-2	-1.6E-3	3.5E-2
l-	SP	100,301	6.4E-7	-1.0E-6	-5.3E-4	-7.8E-4	-2.7E-6
	AP	4,81	8.9E-8	-2.1E-7	-1.1E-4	-1.4E-4	-1.0E-5
	PO	73,127	6.9E-6	-8.7E-6	-2.7E-3	-8.6E-3	9.5E-4
ls	SP	0,31	1.3E-5	2.4E-6	-7.7E-3	2.5E-4	8.4E-4
	AP	95,26	2.2E-6	1.7E-6	3.1E-4	-1.2E-5	6.1E-4
	PO	164,12	1.3E-4	9.7E-5	1.7E-2	-8.2E-4	3.6E-2

Desired DOF	Port	Demod. Phase	L_+	L_-	l_+	l_-	l_s
l+	SP	189,32	-1.7E-3	-3.0E-4	1	-3.2E-2	-1.0E-1
	AP	104,26	7.0E-3	5.4E-3	1	1.8E-3	1.9
	PO	177,12	7.3E-3	5.5E-3	1	-9.5E-2	2.1
l-	SP	100,301	-8.2E-4	1.3E-3	6.8E-1	1	3.4E-3
	AP	4,81	-6.2E-4	1.5E-3	7.5E-1	1	7.1E-2
	PO	73,127	-8.0E-4	1.0E-3	3.1E-1	1	-1.1E-1
ls	SP	0,31	1.5E-2	2.9E-3	-9.2	2.9E-1	1
	AP	95,26	3.6E-3	2.8E-3	5.1E-1	-2.0E-2	1
	PO	164,12	3.6E-3	2.7E-3	4.6E-1	-2.3E-2	1

4. Comparison between various POs

There are three POs possible: light from BS to one of the ITMs, one from BS to PRM, one from PRM to BS. They carry slightly different information from one another.

The contour plots for the three POs are shown in Fig. 5 to Fig. 7. It can be seen that they are very similar in a sense that relative positions of the contours for the signals and dc offset are almost the same.

The matrix for the three POs is shown in Table 4. As expected they are all comparably good matrices. Thus we will stick to the currently-designed PO, which is the light from BS to one of the ITMs.

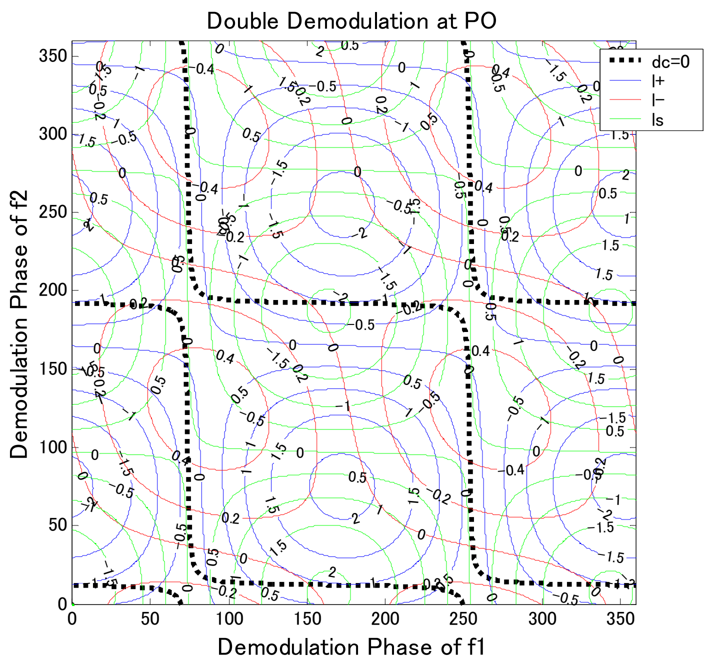

Fig. 5. Dependence of the signals and dc offset at PO (BS to ITM) on the demodulation phases.

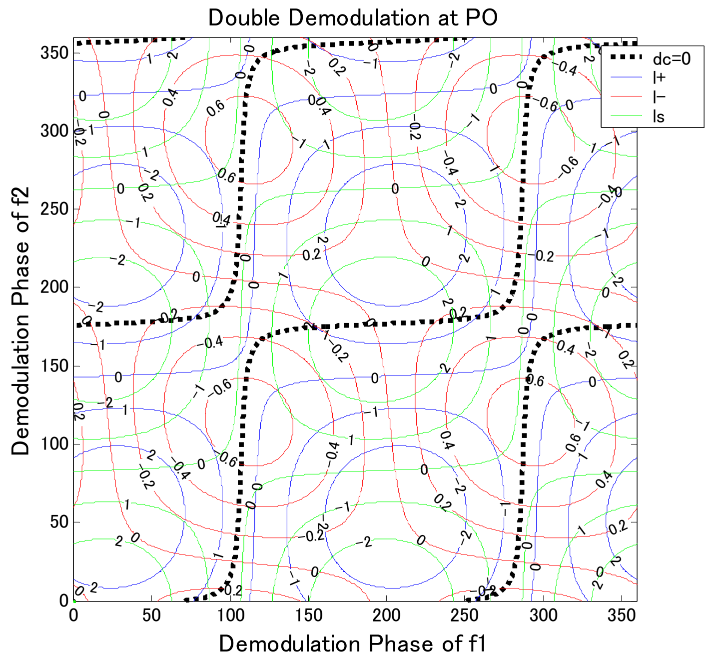

Fig. 6. Dependence of the signals and dc offset at PO (BS to PRM) on the demodulation phases.

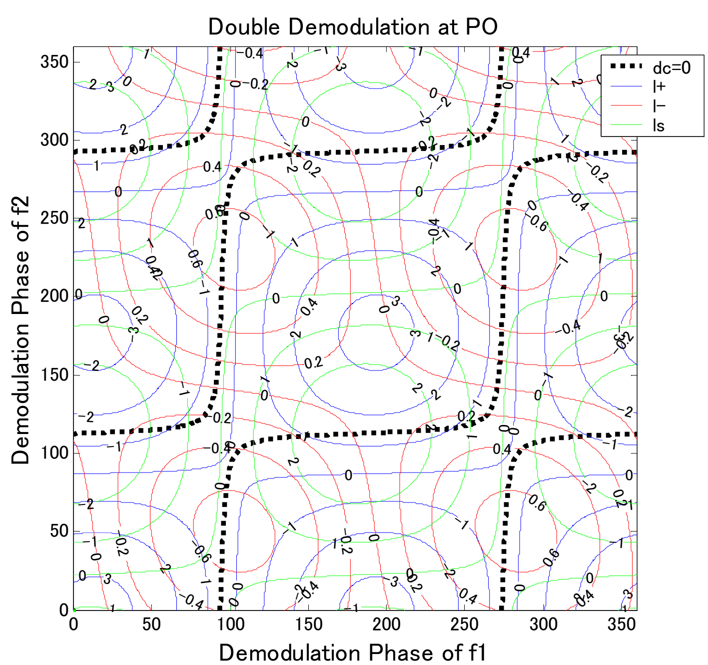

Fig. 7. Dependence of the signals and dc offset at PO (PRM to BS) on the demodulation phases.

Table 4. Comparison of the three PO ports for obtaining the l_+, l_-, and l_s signals
(Upper: Raw value; Lower: Normalized; Yellow zone indicates the actual design.)

Port	Demod. Phase	L_+	L_-	l_+	l_-	l_s
BS to ITM	**164,12**	**1.3E-4**	**9.7E-5**	**1.7E-2**	**-8.2E-4**	**3.6E-2**
BS to PRM	**197,177**	**1.8E-4**	**1.4E-4**	**2.7E-2**	**-5.6E-4**	**5.0E-2**
PRM to BS	**184,113**	**1.8E-4**	**1.4E-4**	**2.5E-2**	**-5.9E-4**	**4.9E-2**

PO Port	Demod. Phase	L_+	L_-	l_+	l_-	l_s
BS to ITM	**164,12**	**3.6E-3**	**2.7E-3**	**4.6E-1**	**-2.3E-2**	**1**
BS to PRM	**197,177**	**3.6E-3**	**2.8E-3**	**5.4E-1**	**-1.1E-2**	**1**
PRM to BS	**184,113**	**3.6E-3**	**2.8E-3**	**5.9E-1**	**-1.2E-2**	**1**

5. Tolerances of cavity length

It is an important question how the signal matrix is affected by the deviation of the macroscopic cavity length from the ideal length.

We start with the signal matrix with the ideal cavity length (Table 5). Then we show the matrix with the l_- length deviation of 2 cm (Table 6) and 6 cm (Table 7), with the l_+ length deviation of 1 cm (Table 8) and 3 mm (Table 9), with the l_s length deviation of 1 cm (Table 10) and 3 mm (Table 11). Here the demodulation phases for the double demodulation are optimized for each length deviation. Incidentally the demodulation phase for single demodulation is optimized to maximize the desired length signal.

Table 5. Signal matrix with the ideal cavity length.
(Upper: Raw value; Lower: Normalized)

Port	Dem. Freq.	Dem. Phase	L_+	L_-	l_+	l_-	l_s
SP	f_1	**10**	**1.9E+1**	**-7.3E-8**	**-2.4E-2**	**-2.4E-5**	**-4.5E-5**
AP	f_2	**271**	**3.6E-9**	**-7.3E-1**	**-8.8E-9**	**-9.2E-4**	**1.2E-8**
SP	$f_1 \times f_2$	**189,32**	**-1.3E-5**	**-2.3E-6**	**7.8E-3**	**-2.5E-4**	**-8.2E-4**
AP	$f_1 \times f_2$	**4,81**	**8.9E-8**	**-2.1E-7**	**-1.1E-4**	**-1.4E-4**	**-1.0E-5**
PO	$f_1 \times f_2$	**164,12**	**1.3E-4**	**9.7E-5**	**1.7E-2**	**-8.2E-4**	**3.6E-2**

Port	Dem. Freq.	Dem. Phase	L_+	L_-	l_+	l_-	l_s
SP	f_1	**10**	**1**	**-3.8E-9**	**-1.2E-3**	**-1.3E-6**	**-2.3E-6**
AP	f_2	**271**	**-4.8E-9**	**1**	**1.2E-8**	**1.3E-3**	**-1.7E-8**
SP	$f_1 \times f_2$	**189,32**	**-1.7E-3**	**-3.0E-4**	**1**	**-3.2E-2**	**-1.0E-1**
AP	$f_1 \times f_2$	**4,81**	**-6.2E-4**	**1.5E-3**	**7.5E-1**	**1**	**7.1E-2**
PO	$f_1 \times f_2$	**164,12**	**3.6E-3**	**2.7E-3**	**4.6E-1**	**-2.3E-2**	**1**

Table 6. Signal matrix with l_{-} of 2 cm
(Upper: Raw value; Lower: Normalized)

Port	**Dem. Freq.**	**Dem. Phase**	L_{+}	L_{-}	l_{+}	l_{-}	l_s
SP	f_1	**11**	**1.7E+1**	**-6.3E-8**	**-2.9E-2**	**-2.2E-5**	**-4.2E-5**
AP	f_2	**270**	**4.7E-9**	**-7.3E-1**	**-1.3E-6**	**-9.2E-4**	**-1.2E-6**
SP	$f_1 \times f_2$	**190,31**	**-1.3E-5**	**-2.7E-6**	**7.8E-3**	**-2.4E-4**	**-1.0E-3**
AP	$f_1 \times f_2$	**5,90**	**9.0E-8**	**-2.1E-7**	**-1.1E-4**	**-1.4E-4**	**-1.1E-5**
PO	$f_1 \times f_2$	**164,12**	**1.2E-4**	**9.2E-5**	**1.6E-2**	**-7.0E-4**	**3.6E-2**

Port	**Dem. Freq.**	**Dem. Phase**	L_{+}	L_{-}	l_{+}	l_{-}	l_s
SP	f_1	**11**	**1**	**-3.7E-9**	**-1.2E-3**	**-1.3E-6**	**-2.5E-6**
AP	f_2	**270**	**-6.4E-9**	**1**	**1.8E-6**	**1.3E-3**	**1.6E-6**
SP	$f_1 \times f_2$	**190,31**	**-1.7E-3**	**-3.4E-4**	**1**	**-3.1E-2**	**-1.3E-1**
AP	$f_1 \times f_2$	**5,90**	**-6.4E-4**	**1.5E-3**	**7.8E-1**	**1**	**7.7E-2**
PO	$f_1 \times f_2$	**164,12**	**3.4E-3**	**2.5E-3**	**4.5E-1**	**-1.9E-2**	**1**

Table 7. Signal matrix with l_{-} of 6 cm
(Upper: Raw value; Lower: Normalized)

Port	**Dem. Freq.**	**Dem. Phase**	L_{+}	L_{-}	l_{+}	l_{-}	l_s
SP	f_1	**12**	**1.2E+1**	**-4.2E-8**	**-1.5E-2**	**-1.4E-5**	**-3.5E-5**
AP	f_2	**270**	**1.7E-9**	**-7.2E-1**	**-6.9E-6**	**-9.0E-4**	**-7.3E-6**
SP	$f_1 \times f_2$	**191,28**	**-1.4E-5**	**-3.1E-6**	**7.6E-3**	**-2.1E-4**	**-1.4E-3**
AP	$f_1 \times f_2$	**5,99**	**7.2E-8**	**-2.3E-7**	**-1.3E-4**	**-1.4E-4**	**-2.4E-5**
PO	$f_1 \times f_2$	**164,12**	**1.1E-4**	**8.1E-5**	**1.5E-2**	**-4.7E-4**	**3.6E-2**

Port	**Dem. Freq.**	**Dem. Phase**	L_{+}	L_{-}	l_{+}	l_{-}	l_s
SP	f_1	**12**	**1**	**-3.4E-9**	**-1.2E-3**	**-1.1E-6**	**-2.8E-6**
AP	f_2	**270**	**-2.4E-9**	**1**	**9.6E-6**	**1.3E-3**	**1.0E-5**
SP	$f_1 \times f_2$	**191,28**	**-1.9E-3**	**-4.0E-4**	**1**	**-2.7E-2**	**-1.8E-1**
AP	$f_1 \times f_2$	**5,99**	**-5.4E-4**	**1.7E-3**	**9.9E-1**	**1**	**1.8E-1**
PO	$f_1 \times f_2$	**164,12**	**3.1E-3**	**2.2E-3**	**4.2E-1**	**-1.3E-2**	**1**

Table 8. Signal matrix with l_+ of 1 cm
(Upper: Raw value; Lower: Normalized)

Port	Dem. Freq.	Dem. Phase	L_+	L_-	l_+	l_-	l_s
SP	f_1	334	2.0E+1	-1.6E-7	-2.5E-2	-8.4E-5	-4.7E-5
AP	f_2	230	6.5E-10	-4.9E-1	-1.5E-8	-6.2E-4	8.4E-9
SP	$f_1 \times f_2$	162,73	-3.9E-6	2.1E-6	6.1E-3	-3.4E-4	7.7E-4
AP	$f_1 \times f_2$	173,218	-1.6E-7	-4.5E-8	2.3E-4	-1.1E-4	2.6E-5
PO	$f_1 \times f_2$	329,153	1.1E-5	2.9E-5	2.8E-2	-1.8E-3	1.1E-2

Port	Dem. Freq.	Dem. Phase	L_+	L_-	l_+	l_-	l_s
SP	f_1	334	1	-7.6E-9	-1.2E-3	-4.1E-6	-2.3E-6
AP	f_2	230	-1.3E-9	1	3.0E-8	1.3E-3	-1.7E-8
SP	$f_1 \times f_2$	162,73	-6.5E-4	3.5E-4	1	-5.6E-2	1.3E-1
AP	$f_1 \times f_2$	173,218	1.5E-3	4.2E-4	-2.1	1	-2.4E-1
PO	$f_1 \times f_2$	329,153	1.1E-3	2.7E-3	2.6	-1.6E-1	1

Table 9. Signal matrix with l_+ of 3 mm
(Upper: Raw value; Lower: Normalized)

Port	Dem. Freq.	Dem. Phase	L_+	L_-	l_+	l_-	l_s
SP	f_1	359	1.9E+1	-9.7E-8	-2.3E-2	-4.2E-5	-4.5E-5
AP	f_2	255	2.3E-9	-6.8E-1	-6.5E-8	-8.6E-4	5.3E-9
SP	$f_1 \times f_2$	179,30	-1.0E-5	1.0E-7	8.6E-3	-3.7E-4	9.4E-5
AP	$f_1 \times f_2$	1,68	4.6E-8	-1.2E-7	2.2E-5	-1.4E-4	1.6E-5
PO	$f_1 \times f_2$	338,178	1.0E-4	8.2E-5	2.1E-2	-8.7E-4	3.0E-2

Port	Dem. Freq.	Dem. Phase	L_+	L_-	l_+	l_-	l_s
SP	f_1	359	1	-5.1E-9	-1.2E-3	-2.2E-6	-2.4E-6
AP	f_2	255	-3.3E-9	1	9.4E-8	1.3E-3	-7.7E-9
SP	$f_1 \times f_2$	179,30	-1.2E-3	1.2E-5	1	-4.4E-2	1.1E-2
AP	$f_1 \times f_2$	1,68	-3.3E-4	9.0E-4	-1.6E-1	1	-1.2E-1
PO	$f_1 \times f_2$	338,178	3.4E-3	2.7E-3	6.9E-1	-2.9E-2	1

Table 10. Signal matrix with l_s of 1 cm
(Upper: Raw value; Lower: Normalized)

Port	Dem. Freq.	Dem. Phase	L_+	L_-	l_+	l_-	l_s
SP	f_1	9	1.9E+1	-7.0E-8	-2.3E-2	-2.3E-5	-4.5E-5
AP	f_2	230	2.4E-10	-4.9E-1	6.7E-8	-6.2E-4	2.8E-8
SP	$f_1 \times f_2$	189,68	-5.0E-6	2.1E-6	6.9E-3	-2.4E-4	8.0E-4
AP	$f_1 \times f_2$	4,40	6.7E-8	-1.3E-7	-6.5E-5	-9.7E-5	-2.8E-6
PO	$f_1 \times f_2$	342,155	9.6E-6	2.6E-5	2.6E-2	-1.1E-3	1.0E-2

Port	Dem. Freq.	Dem. Phase	L_+	L_-	l_+	l_-	l_s
SP	f_1	9	1	-3.6E-9	-1.2E-3	-1.2E-6	-2.3E-6
AP	f_2	230	-4.8E-10	1	-1.4E-7	1.3E-3	-5.6E-8
SP	$f_1 \times f_2$	189,68	-7.3E-4	3.1E-4	1	-3.5E-2	1.2E-1
AP	$f_1 \times f_2$	4,40	-6.9E-4	1.4E-3	6.7E-1	1	2.9E-2
PO	$f_1 \times f_2$	342,155	9.2E-4	2.5E-3	2.5	-1.0E-1	1

Table 11. Signal matrix with l_s of 3 mm
(Upper: Raw value; Lower: Normalized)

Port	Dem. Freq.	Dem. Phase	L_+	L_-	l_+	l_-	l_s
SP	f_1	10	1.9E+1	-7.3E-8	-2.3E-2	-2.5E-5	-4.5E-5
AP	f_2	255	2.8E-9	-6.8E-1	1.8E-8	-8.6E-4	5.6E-8
SP	$f_1 \times f_2$	189,30	-9.9E-6	2.2E-7	8.5E-3	-2.9E-4	1.1E-4
AP	$f_1 \times f_2$	4,66	8.8E-8	-1.9E-7	-9.8E-5	-1.3E-4	-7.6E-6
PO	$f_1 \times f_2$	163,358	9.7E-5	7.8E-5	2.0E-2	-1.3E-3	2.9E-2

Port	Dem. Freq.	Dem. Phase	L_+	L_-	l_+	l_-	l_s
SP	f_1	10	1	-3.8E-9	-1.2E-3	-1.3E-6	-2.3E-6
AP	f_2	255	-4.2E-9	1	-2.7E-8	1.3E-3	-8.2E-8
SP	$f_1 \times f_2$	189,30	-1.2E-3	2.6E-5	1	-3.3E-2	1.3E-2
AP	$f_1 \times f_2$	4,66	-6.5E-4	1.4E-3	7.3E-1	1	5.6E-2
PO	$f_1 \times f_2$	163,358	3.3E-3	2.6E-3	6.8E-1	-4.3E-2	1

A cross coupling of greater than unity in the normalized matrix is not desirable (highlighted in red). From the Tables the cavity length tolerances are: approximately 6 cm for l_- and somewhere between 3 mm and 1 cm for l_+ and l_s.

4. Conclusions

It can be recommended that double demodulation should be used for obtaining all the small l signals. We may as well stick to the default port allocation (l_+ at SP, l_- at AP, and l_s at PO), and stick to the currently-designed PO (from BS to one of the ITMs). The acceptable cavity length deviations from the ideal points are 6 cm for l_-, 3 mm for l_+, and 3 mm for l_s.

Appendix A

Optical parameters used in FINESSE are as follows:

Laser Power: 1 W
f1: f = 33.2066 MHz, M = 0.1, up to 3rd order SB)
f2: f = 166.033 MHz, M = 0.1, up to 3rd order SB)

PRM: T = 70000 ppm, L = 37.5 ppm
SEM: T = 70000 ppm, L = 37.5 ppm, Detuned phase = 21.186°
ITM: T = 5000 ppm, L = 37.5 ppm
ETM: T = 10 ppm, L = 37.5 ppm
BS: R = 0.4995, T = 0.4995
L(PRM-BS): 0.3 m
L (SEM-BS): 0.1937392798 m
L (BS-ITM1): 2.182727107 m
L (BS-ITM2): 1.731322178 m
L (ITM1-ETM1): 38.448 m
L (ITM2-ETM2): 38.652 m